Published in final edited form as:

Neurobiol Dis. 2014 March ; 63: 171–183. doi:10.1016/j.nbd.2013.12.002.

Prodegenerative IκBα expression in oligodendroglial α-synuclein models of multiple system atrophy

Christine L. Kragh[1], **Amanda M. Gysbers**[2], **Edward Rockenstein**[3], **Karen Murphy**[2], **Glenda M. Halliday**[2], **Eliezer Masliah**[3], and **Poul Henning Jensen**[1]

[1]Department of Biomedicine & Danish Research Institute of Translational Neuroscience - DANDRITE, University of Aarhus, Aarhus, Denmark, School of Medicine, La Jolla, California 92093-0624

[2]Neuroscience Research Australia and University of New South Wales, Sydney, NSW, Australia, School of Medicine, La Jolla, California 92093-0624

[3]Department of Neurosciences and Pathology, University of California, San Diego, School of Medicine, La Jolla, California 92093-0624

Abstract

Multiple system atrophy is a progressive, neurodegenerative disease characterized by parkinsonism, ataxia, autonomic dysfunction, and accumulation of α-synuclein in oligodendrocytes. To understand how α-synuclein aggregates impact oligodendroglial homeostasis, we investigated an oligodendroglial cell model of α-synuclein dependent degeneration and identified responses linked to the NF-κB transcription factor stress system. Coexpression of human α-synuclein and the oligodendroglial protein p25α increased the expression of IκBα mRNA and protein early during the degenerative process and this was dependent on both aggregation and Ser129 phosphorylation of α-synuclein. This response was prodegenerative because blocking IκBα expression by siRNA rescued the cells. IκBα is an inhibitor of NF-κB and acts by binding and retaining NF-κB p65 in the cytoplasm. The protection obtained by silencing IκBα was accompanied by a strong increase in nuclear p65 translocation indicating that NF-κB activation protects against α-synuclein aggregate stress. In the cellular model, two different phenotypes were observed; degenerating cells retracting their microtubules and resilient cells tolerating the coexpression of α-synuclein and p25α. The resilient cells displayed a significant higher nuclear translocation of p65 and activation of the NF-κB system relied on stress elicited by aggregated and Ser129 phosphorylated α-synuclein. To validate the relationship between oligodendroglial α-synuclein expression and IκBα, we analyzed two different lines of transgenic mice expressing human α-synuclein under the control of the oligodendrocytic MBP promotor (intermediate-expresser line 1 and high-expresser line 29). IκBα mRNA expression was increased in both lines and immunofluorescence microscopy and *in situ* hybridization revealed that IκBα mRNA and protein is expressed in oligodendrocytes. IκBα mRNA expression was demonstrated prior to activation of microglia and astrocytes in line 1. Human brain tissue affected by MSA displayed increased expression of IκBα and NF-κB p65 in some oligodendrocytes containing glial cytoplasmic inclusions.

To whom correspondence should be addressed: Professor Poul Henning Jensen, Tel: +45 8716 7793; phj@biokemi.au.dk.

Our data suggest that oligodendroglial IκBα expression and NF-κB is activated early in the course of MSA and their balance contributes to the decision of cellular demise. Favoring oligodendroglial NF-κB activation may represent a therapeutic strategy for this devastating disease.

Keywords

multiple system atrophy; NF-κB; IκBα; α-synuclein; oligodendrocytes

Introduction

Multiple system atrophy (MSA) is the collective term for three previous perceived independent diseases olivopontocerebellar degeneration, striatonigral degeneration and Shy-Drager syndrome (Burn and Jaros, 2001). The reason for combining these disorders into one entity was the recognition of glial cytoplasmic inclusions (GCIs) in oligodendrocytes as a common cytopathological denominator despite their different clinical manifestations (Jellinger, 2003; Papp et al., 1989; Wakabayashi and Takahashi, 2006; Yoshida, 2007). The demonstration of α-synuclein (α-syn) aggregates in GCIs placed MSA within the groups of synucleinopathies, dominated by Parkinson's disease (PD) and Dementia with Lewy bodies that apart from MSA are characterized by neuronal intracellular α-syn inclusions, Lewy bodies (Gai et al., 1999; Wakabayashi et al., 1998). Missense mutations within and multiplications of the normal coding region of the α-syn gene cause autosomal dominant PD and DLB (Farrer et al., 2004; Kruger et al., 2002; Polymeropoulos et al., 1997; Singleton et al., 2003; Zarranz et al., 2004). This demonstrates that α-syn dysmetabolism directly induces PD and DLB and initiate neuropathology covering the various Braak stages of PD. GCIs have recently been demonstrated in a family carrying a mutation in the α-syn gene (G51D) (Kiely et al., 2013) indicating that both α-syn and other factors may be causing MSA. The massive oligodendroglial accumulation of aggregated α-syn (Dickson et al., 1999; Jellinger, 2003) formed the basis for generation of several transgenic mice expressing human α-syn under the control of oligodendroglial promoters (Kahle et al., 2002; Shults et al., 2005; Yazawa et al., 2005). These mice show that oligodendroglial expression of human α-syn results in the formation of α-syn-containing GCIs, myelin damage, astrogliosis and glial and neuronal loss. The mechanisms associated with this cellular damage are yet to be determined.

The NF-κB family of transcription factors represents a conserved stress signaling system (Lenardo and Baltimore, 1989) that plays a central role in inflammatory responses (Lawrence, 2009). The dominating NF-κB transcription factors in brain are the dimeric p65 and p50 proteins and their nuclear access is negatively regulated by binding to cytosolic IκB inhibitory proteins. NF-κB inducing stimuli activate IκB kinase complexes that destabilize IκB proteins (reviewed in (Papa et al., 2004)). The NF-κB system is active in brain and can play a protective function in neurons (Kaltschmidt and Kaltschmidt, 2009) but its role in brain disorders is less clear although it can display opposing cell type specific functions, e.g. protective function in oligodendrocytes (Bonetti et al., 1999) and degenerative function in astrocytes (Raasch et al., 2011).

The functional involvement of the NF-κB system in synucleinopathies is not known but the p65 subunit has been identified in nuclei of midbrain dopaminergic neurons and Lewy body inclusions in PD and DLB (Ghosh et al., 2007; Hunot et al., 1997; Noda et al., 2005; Soos et al., 2004; Togo et al., 2001) and destabilized phosphorylated inhibitor IκBa is localized in Lewy bodies (Noda et al., 2005)..

The present study is based on a cellular model of MSA (Kragh et al., 2009) wherein the NF-κB inhibitor IκBa is expressed early during the course of α-syn aggregation dependent degeneration. The model demonstrates two cellular phenotypes, α-syn dependent degeneration and resilience that is dependent on successful cytoprotective NF-κB activation or its negative regulation by IκBα. The cellular IκBα response is initiated by α-syn aggregation and Ser129-phosphorylation dependent processes. Investigations of transgenic mice expressing α-syn in mature oligodendrocytes regulated by the MBP promoter allowed validation of cell autonomous IκBα expression in α-syn expressing oligodendrocytes as an early phenomenon *in vivo*. Studies of human MSA tissue revealed a complex cellular response with increased IκBα expression and NF-κB activation in α-syn containing oligodendrocytes besides strong astrocytic IκBα expression. Conclusively, the data suggest that modification of oligodendrocytic NF-κB activity in MSA may represent a novel therapeutic strategy.

Materials and Methods

Cell cultures

OLN-93 is an immortalized oligodendroglia cell line derived from primary Wistar rat brain glial cultures (Richter-Landsberg and Heinrich, 1996). From these cells, two clones were established, first OLN-t40 cells expressing the longest human tau isoform (Tau40) and subsequently the double transfected OLN-t40-AS cells also expressing human α-syn (Kragh et al., 2009). OLN-93 cells and OLN-t40 cells were in the present study used as negative controls for α-syn aggregate dependent effects in α-syn transfected OLN-93 and OLN-t40-AS cells. For inhibition of α-syn aggregation, cells were treated with 10 μM ASI1D peptide (El Agnaf et al., 2004) (synthesized by Schafer-N, Copenhagen, Denmark) for 1 h before transfection with p25α. For inhibition of NF-κB signaling, 5–20 μM of Ikkγ NEMO Binding Domain (NBD) inhibitor peptide (Imgenex, San Diego, CA) was added to the cells 4 h after transfection with p25α. NBD peptide contains a protein transduction (PTD) sequence derived from antennapedia; the control peptide consists of only the PTD sequence.

Plasmids, transfection and siRNA silencing

pcDNA3.1 zeo(−) plasmids expressing human wild-type (wt) α-syn, α-syn S129A, and p25α were produced as previously described (Kragh et al., 2009). Transient transfections of cells were performed with Fugene-6 Transfection Reagent according to the manufacturer's protocol (Roche, Mannheim, Germany). Experiments requiring high transfection efficiencies were performed with Amaxa® Cell Line Nucleofector Kit V according to the manufacturer's protocol (Lonza, Basel, Switzerland).

ON-TARGETplus siRNA SMARTpool comprising four siRNAs targeting rat IκBα was purchased from Dharmacon (Lafayette, CO, USA). siControl pool comprising four non-targeting siRNAs was included as a negative control. Transfection of siRNA into OLN-t40-AS cells was performed using Dharmafect Transfection Reagent 1 according to the manufacturer's instructions. In brief, 100 nM siRNA pool was transfected into OLN-t40-AS cells using 1 μl Dharmafect Transfection Reagent 1 for cells in each well of 24-well plates. Efficient siRNA-mediated silencing was confirmed by real-time qPCR. The effect of gene silencing on p25α-transfected OLN-t40-AS cells was evaluated by transfecting the cells with siRNA for 72 h followed by transient transfections with p25α. MT retraction was analyzed 24 h after p25α-transfection.

Transgenic mice and tissue processing

Mice expressing human α-syn under control of the MBP promotor were generated as described (Shults et al., 2005). Genomic DNA was extracted from tail biopsies and analyzed by PCR as described. In this study, we used MBP-hα-syn line 1 and 29 (3 months, n=6), which express an intermediate and a high level of α-syn, respectively. Both lines have previously been shown to accumulate α-syn in oligodendrocytes and to display neuropathological alterations including myelin loss and astrogliosis and behavioral deficits (Shults et al., 2005).

Following NIH guidelines for the humane treatment of animals, mice were killed under anesthesia and brains were removed. The right hemibrain was immersion-fixed in 4% paraformaldehyde in PBS pH 7.4, and serially sectioned at 40 μm with a Vibratome (Leica). The left hemibrain was kept at −80°C for biochemical analysis.

Human brain samples and tissue processing

Approval was obtained to assess frozen human brain tissue from five MSA cases (four MSA-C (cerebellar type) and one MSA-P (Parkinsonian type) and five age-matched controls, collected with consent and ethics approval through the South Australian and Sydney Brain Banks. MSA cases were autopsy confirmed and controls had no significant neuropathology and no evidence of neurological or psychiatric disease. None of the cases had brain injury due to non-degenerative mechanisms (such as head trauma, infarction or sepsis) or other significant neuropathological changes. All cases were collected within 36 h of death. The average (± S.D.) age of the MSA group was 73±7 years with an average duration of MSA of 4±3 years and an average post-mortem delay of 11±7 hrs. The average age of the control group was 71±7 years and the average post-mortem delay was 14±6.5 hrs.

Half of the hemisphere was freshly sectioned and frozen blocks stored at −80°C prior to fractionation. Brain tissue from white matter under the precentral gyrus (as this region contains GCIs but does not contribute to clinical presentation and is without substantial atrophy and degeneration) was used for analysis.

Immunocytochemistry

Cells were cultured on PLL-coated coverslips. For analysis, cells were fixed with 4% paraformaldehyde for 15 min, permeabilized with 0.1% Triton X-100 for 30 min, and

blocked in 3% BSA solution for 20 min at room temperature (RT). Cell preparations were incubated with primary antibodies for 1 h at RT and proteins were visualized by Alexa Fluor 488 or −568 conjugated secondary antibodies (Invitrogen, Leiden, The Netherlands). Nuclei were stained by 4´,6-diamidino-2-phenylindole (DAPI). Signals were analyzed by epifluorescence microscopy (Axiovert 200M, Zeiss, Germany) or by confocal microscopy (LSM710, Zeiss, Germany).

Assessment of NF-κB translocation and microtubule retraction in cells

Immunocytochemistry was performed on cultured cells to directly visualize the translocation of NF-κB from the cytoplasm to the nucleus. Cells were immunostained for α-tubulin, p25α, and NF-κB p65, counterstained with DAPI, and analyzed by fluorescence microscopy. NF-κB translocation was quantified by counting the number of transfected cells with a clear localization of NF-κB in the nucleus as compared to the total number of transfected cells. In each experiment, 100-200 transfected cells were examined at 400 times magnification.

MT retraction was quantified as described previously (Kragh et al., 2009) and defined as retraction of MT from the cellular processes to the perinuclear region resulting in an intense α-tubulin staining surrounding the nucleus. MT retraction was quantified by counting p25α-positive cells with a clear perinuclear localization of MT compared to the total number of p25α-positive cells. In each experiment, 100–200 transfected cells localized in randomly chosen microscopic fields were examined at 100 times magnification.

RNA isolation and real-time qPCR

Isolation of total RNA was performed using RNeasy Mini Kit (Qiagen) for cell culture and RNeasy Lipid Mini Kit (Qiagen) for mouse tissue according to the manufacturer´s instructions. All samples were treated with DNase I to eliminate genomic DNA contamination. Purity and integrity of isolated RNA was checked spectrometrically and by agarose gel electrophoresis. Reverse transcription was performed using the High Capacity cDNA Reverse Transcription Kit according to the manufacturer´s protocol (Applied Biosystems, Foster City, CA, USA). 0.5 μg of the extracted RNA was used for cDNA production. Real-time qPCR assays were performed in triplicates using the 7500 Fast Real-Time PCR System (Applied Biosystems) in a 96-well format. Each reaction contained 10 μl 2× Fast SYBR Green Master Mix (Applied Biosystems), 200 nM of forward and reverse primers, 7 μl nuclease-free H_2O, and 2 μl cDNA in a final volume of 20 μl. Expression levels were normalized to NADH mRNA (cell culture) or GAPDH (mouse tissue) and calculated using the $\Delta\Delta C_T$-method (SDS1.4 Software, Applied Biosystems).

Affymetrix gene chip analysis of genes induced by cellular co-expression of α-synuclein and p25α

α-Syn aggregate dependent IκBα gene expression was first observed in a microarray analysis of gene expression performed to identify putative transcriptional responses to aggregated α-syn. Biotinylated cRNA from two independent transfections of OLN-t40-AS cells stably expressing human α-syn with an empty vector or p25α for 8, 12, and 16 h were hybridized to Affymetrix RAE 230 2.0 Gene Chips at Molecular Diagnostic Laboratory, Aarhus University Hospital, Denmark.. The Affymetrix RAE230 2.0 oligonucleotide array

contains approximately 31,000 probe sets. Each gene is represented by 11 pairs of 25 mer sequence probes that contain a perfectly matched probe and a mismatched probe, which serve as controls for background signals. The raw image files from the quantitative scanning were analyzed by Gene Expression Analysis Software (MAS 5.0) (Affymetrix) resulting in CEL files containing background corrected probe values. The two identical independent experiments were performed in mock-versus p25α-transfected OLN-t40-AS cells resulting in a total of twelve arrays. To identify genes that were differential expressed between the two conditions, the data set was filtered according to several criteria. i) The dataset was filtered by the Detection Call (Present (P), Marginal (M), or Absent (A)). ii) Probe sets that were either increasing to an absent call or decreasing from an absent call were excluded from the dataset. iii) Data were included only if at least one of the signal levels in a comparison was ≥ 50. iv) Genes with no name or annotation were excluded from the data set. v) Remaining data were included only if the absolute change in signal level was ≥ 1.3-fold. Using these criteria 104 genes (91 up-regulated genes and 13 down-regulated genes) were identified as exemplified in Table 1. The identified genes could be the result of expression of p25α or the generation of misfolded α-syn by coexpressing α-syn and p25α. Hence validation experiments were conducted for selected genes where p25α was expressed in the parental OLN-93 cell line with empty vector and co-expressed with α-syn vector. The selection of IκBα for this study was based on its possible prodegenerative function.

Immunohistochemistry

Immunohistochemistry analysis was performed on 40μm free-floating vibratome sections from ntg and MBP-hα-syn tg mice (n=6). After rinsing in PBS (3×5 min), sections were treated with 5% H_2O_2/0.1% Tween-20 and incubated with 10% normal serum. After rinsing in PBS (3×5 min), sections were incubated overnight with antibodies against the astroglial marker glial fibrillary acidic protein (GFAP; Millipore, Temecula, CA) or the microglial marker ionized calcium-binding adaptor molecule-1 (Iba1; Wako, Richmond, VA). Excess primary antibody was rinsed from the sections with PBS (3×5 min) and sections were incubated with biotinylated secondary antibodies (Vector Laboratories) for 60 min. An amplification step was conducted by incubating sections in ABC mixture (ABC Vectrastain Elite, Vector Laboratories Inc, Burlingame, CA) for 60 min followed by PBS washes. Sections were exposed to diaminobenzidine tetrahydrochloride (DAB), transferred to SuperFrost slides (Thermo Fisher Scientific) and mounted under glass coverslips before analysis under a light microscope.

Double-labeling immunofluorescence

Double-labeling immunofluorescence on mouse tissue was performed on 40μm free-floating sections from ntg (n=3) and MBP-hα-syn tg mice (n=3). For this purpose, sections were immunolabeled overnight with a rat polyclonal antibody against the oligodendroglial marker p25α (produced in-house) in combination with mouse monoclonal anti-α-syn (Syn211, Millipore) or rabbit polyclonal anti-IκBα (Santa Cruz Biotechnology). Immunoreactive structures were detected with AlexaFluor-conjugated antibodies (Molecular Probes). All primary and secondary antibodies were diluted in PBS pH 7.4. Sections were imaged using a Zeiss LSM-710 confocal microscope system (Carl Zeiss MicroImaging GmbH, Germany).

Double-labeling immunofluorescence on human tissue was performed on 10μm formalin-fixed paraffin-embedded sections from the pontine white matter from MSA patients (n=2) and controls (n=2). Sections were deparaffinized in xylene and rehydrated in graded ethanol. Antigen retrieval was performed using 90% formic acid for 3 min (for detection of α-syn) and boiling in 1% antigen unmasking solution (Vector Laboratories) in the microwave for 10 min (for NF-κB, IκBα and p25α detection). Slides were treated with 5% H_2O_2/50% ethanol, blocked in 10% normal horse serum and incubated with primary antibodies for 72 hrs. The primary antibodies were mouse monoclonal anti-α-syn (mAb42, Transduction Labs), mouse monoclonal anti-NF-κB p65 (F-6, Santa Cruz Biotechnology), rabbit polyclonal anti-IκBα (C-21, Santa Cruz Biotechnology), mouse monoclonal anti-GFAP (DAKO), rabbit polyclonal anti-GFAP (Sigma) and rat polyclonal anti-p25α (produced in-house). All primary and secondary antibodies were diluted in 0.1M Tris buffer. After washing, sections were incubated in AlexaFluor-conjugated secondary antibodies for 2 h at RT.

In situ hybridization

Antisense and sense oligonucleotide probes were generated against mouse IκBα and the probes were labeled with digoxigenin using the DIG Oligonucleotide Tailing Kit 2nd generation (Roche) according to the manufacturer´s instructions. Paraffin sections from ntg and MBP-hα-syn tg mice were prepared for *in situ* by deparaffinization through xylene and rehydration in graded ethanol. Sections were treated with proteinase K [5 ug/ml), incubated in prehybridization solution (2× standard saline citrate (SSC), 10% dextran sulfate, 0.02% SDS, 50% formamide, 1% blocking reagent (Roche), 100 μg/ml salmon sperm DNA (Sigma)] and hybridized with 30 nmol/l of each digoxigenin-labeled oligonucleotide probe at 37°C overnight. Sections were processed through stringent posthybridization washes (2×SSC; 2×SSC/50% formamide, 1×SSC, 0.25×SSC) and processed for immunodetection of digoxigenin with anti-DIG antibody conjugated to alkaline phosphatase (Roche). NBT/BCIP precipitates were observed under a light microscope.

Western blot analysis

Protein levels of NF-κB p65 and IκBα in OLN cells were determined by western blot analysis of total cell extracts as previously described (Kragh et al., 2009). Primary antibodies were anti-NF-κB p65 (C-20, Santa Cruz Biotechnology), anti-IκBα (C21, Santa Cruz Biotechnology), ASY1(Lindersson et al., 2005), anti-α-tubulin (Sigma, Steinheim, Germany), and anti-p25α (Lindersson et al., 2005). For detection, membranes were probed with HRP-conjugated secondary antibodies, and proteins were visualized with enhanced chemiluminescence (ECL) using a Fuji Las-3000 imager. Protein bands were quantified using the MultiGauge software (Fuji LAS-3000).

Protein levels of IκBα and NF-κB p65 in mouse brain tissue were analyzed by western blot analysis in soluble fractions of mouse brain homogenates as described in (Shults et al., 2005). 20 ug total protein from cytosolic fractions was loaded onto 4–12% Bis-Tris SDS-PAGE gels (Invitrogen) and transferred onto Immobilon membranes. Membranes were blocked with 5% BSA/PBS-T and incubated with rabbit polyclonal anti-IκBα, rabbit polyclonal anti-NF-κB p65 (Santa Cruz Biotechology), or mouse monoclonal anti-β-actin (Sigma-Aldrich). After overnight incubation with primary antibodies, membranes were

incubated with appropriate secondary antibodies, reacted with ECL, and developed on a VersaDoc gel-imaging instrument (Bio-Rad).

Human tissue was homogenized in homogenization buffer [0.32M sucrose, 20mM Tris-HCl pH 7.4, 5mM EDTA, 1× protein inhibitor cocktail (EDTA free; Roche), 1× phosphatase inhibitor (Roche)], sonicated 2 × 10s on ice where after soluble proteins were isolated in the supernatant after centrifugation at 23,500g for 10min at 4°C. The insoluble fraction was washed twice with homogenization buffer, and extracted in SDS-urea solubilisation buffer (6M urea, 1% SDS, 5mM EDTA) (1:5 w/v), sonicated for 2 × 10s and centrifuged at 23,500g for 10min. The supernatant representing the urea-SDS soluble fraction was referred to as the insoluble fraction.

All protein concentrations were determined using the BCA method (Pierce). 20 μg of tissue extract was separated by SDS-PAGE and transferred onto polyvinylidene difluoride (PVDF) membranes. Membranes were blocked with 5% powdered skim milk in TBS-T (10mM Tris-HCl, pH 7.5, 150mM NaCl and 0.05% Tween-20) for 2 h. Membranes were probed overnight using primary antibodies diluted in blocking buffer (anti-mouse α-syn (BD Transduction Labs) at 1:500, anti-mouse NF-κB (Santa Cruz Biotechnology) at 1:200, anti-rabbit IκBα (Santa Cruz Biotechnology) at 1:1000, and anti-mouse β-actin (Sapphire Biosciences) at 1:10,000). Membranes were washed three times in TBS-T buffer and probed with HRP-conjugated secondary antibodies diluted in blocking buffer for 1 h at RT (goat anti-mouse IgG-HRP (1:12,000; BioRad Laboratories, Hercules, USA) and goat anti-rabbit IgG-HRP (1:10,000; Sigma-Aldrich, St Louis, USA). Immunoreactivity was visualized by chemiluminescence using an ECL detection system (GE Healthcare Biosciences, Pittsburg, USA) captured onto Hyperfilm (GE Healthcare Biosciences, Pittsburg, USA). Films were scanned and the intensity of each band was quantified using NIH Image J software (National Institutes of Health, Bethesda, MD) with expression normalized to β-actin.

Statistical analyses

Statistical analyses were performed using SPSS (IBM SPSS Statistics 18, Somers, New York, USA) or GraphPad Prism 5.0 (GraphPad Software, La Jolla, USA). Differences between groups were analyzed by unpaired t-tests and a p value less than 0.05 accepted as significant. Averages and standard deviations are given for all values.

Results

α-Synuclein aggregates enhance IκBα expression

MSA is characterized by accumulation of α-syn and p25α within inclusions in degenerating oligodendrocytes. To model the disorder, we developed a cellular model wherein human α-syn and p25α are coexpressed in rat oligodendroglial OLN-93 cell lines, which can be done by transient expression of p25α in the OLN-t40-AS line stably expressing human α-syn or by transient expression of the two transgenes in wild type OLN-93 cells (Kragh et al., 2009). This causes a degenerative phenotype where a rapid reorganization of the MT cytoskeleton takes place within the first 24 h of coexpressing the transgenes (Fig. 1A). This is followed by an induction of apoptosis during the following 24–48 h. Both early and late phases are

dependent on α-syn aggregation and phosphorylation at Ser129 (Kragh et al., 2009). As only 60% of the cells coexpressing α-syn and p25α displayed cellular degeneration, we speculated whether a cytoprotective response was active in the remaining transfected cells.

To identify putative transcriptional responses to aggregated α-syn, we performed microarray analysis of gene expression. Biotinylated cRNA from two independent transfections of OLN-t40-AS cells with an empty vector or with p25α for 8, 12, and 16 h were hybridized to Affymetrix RAE 230 2.0 Gene Chips. By choosing these early time points we were able to identify early cellular responses to aggregated α-syn as exemplified in Table 1. Functional classification of identified genes was based on Gene Ontology categories and was performed by using the publicly available databases: DAVID, Affymetrix, and NCBI. This enabled the identification of the NF-κB pathway as potentially affected in the model based on its inhibitor of NF-κB named IκBα and the response gene IL6. The transcription factor NF-κB p65 promotes the expression of a variety of target genes (Papa et al., 2004) and has been implicated in PD where it translocates to the nucleus of midbrain dopaminergic neurons (Ghosh et al., 2007; Hunot et al., 1997).

IκB family members are inhibitors of NF-κB activation and act by binding and sequestrating NF-κB in the cytoplasm (Papa et al., 2004). We examined the levels of IκBα mRNA (Fig. 1B) as well as protein (Fig. 1C and D) in OLN cells 24 h after transfection. OLN-93 cells were transfected with α-syn wt or α-syn S129A in combination with an empty vector control or p25α vector followed by analysis of mRNA and total cellular protein levels. IκBα mRNA levels were significantly increased in cells coexpressing α-syn wt and p25α as compared to mock-transfected cells (Fig. 1B). mRNA induction was translated into an increase in IκBα protein in total cell extracts from cells coexpressing α-syn and p25α for 24 h as compared to mock-transfected cells (Fig. 1C and D). The temporal induction was rapid as demonstrated by a 2.5-fold increase in IκBα mRNA already 8 h after transfection of α-syn and p25α into OLN cells (Table 1). The degenerative stress in this model relies on phosphorylation of Ser129 and aggregation of α-syn (Kragh et al., 2009). To determine if the same stress parameters are critical for the IκBα mRNA induction we coexpressed α-syn S129A and p25α and treated cells expressing α-syn wt and p25α with the aggregation inhibitor ASI1D (El Agnaf et al., 2004). Both treatments attenuated IκBα mRNA expression after 24 h (Fig. 1B) demonstrating α-syn aggregation and α-syn Ser129 phosphorylation are involved in IκBα induction.

NF-κB translocation is protective in oligodendroglial cells

To demonstrate a functional role for IκBα in α-syn-mediated degeneration, we used siRNA to silence IκBα in OLN-t40-AS cells. A pool of four different siRNAs targeting rat IκBα was transfected into OLN-t40-AS cells 72 h prior to analysis. siControl pool comprising four non-targeting siRNAs was included to control for off-target effects. Gene silencing by siRNA was confirmed by real-time qPCR, which demonstrated a 94% reduction in IκBα mRNA level (data not shown). An effect of gene silencing on cellular degeneration was quantified 24 h after siRNA-treated cells had been transfected with p25α. Fig. 2A demonstrates that p25α caused MT retraction in approximately 60% of the siControl-transfected cells. However, treatment with the siRNA pool targeting IκBα decreased MT

retraction by nearly 70%. Moreover, the NF-κB transcription factor p65, which IκBα sequester in the cytosol, was significantly translocated into the nucleus in these cells as compared to siControl-transfected cells (Fig. 2A). These results demonstrate a direct role of IκBα in α-syn-mediated degeneration and suggest a protective function of nuclear NF-κB p65.

Activation of the kinase IKK is essential for allowing NF-κB p65 to activate its target genes by phosphorylation of IκBα that lead to its subsequent ubiquitination and degradation (Papa et al., 2004). Given that activation of IKKs requires recruitment of NEMO, we treated cells with a cell permeable Nemo binding domain (NBD) peptide to sequester NEMO and thus prevent its binding to IKKγ and inhibition of NF-κB activation. We treated OLN cells coexpressing α-syn and p25α with NBD peptide and quantified MT retraction and NF-κB p65 translocation in the transfected cells. Our results show that NBD peptide (10 and 20 μM) enhances MT retraction in the transfected cells, whereas the control peptide fails to do so (Fig. 2B). The NBD peptide did not result in a significant reduction in the fraction of cells with nuclear translocation of p65. The change in MT retraction was not associated with altered levels of NF-κB p65 protein as demonstrated by western blot analysis of total cell extracts (Fig. 2C). Hence, an increased level of IκBα is associated with α-syn dependent degeneration of oligodendroglial cells.

NF-κB translocation is accompanying α-synuclein-mediated cytotoxicity

We investigated a possible involvement of the NF-κB transcription factor p65 in our cellular model of α-syn-mediated toxicity. NF-κB activation was visualized by translocation of p65 from the cytoplasm to the nucleus (Fig. 3A and B) and functionally determined by expression of the NF-κB activated target gene IL6 (Fig. 3D).

Transient transfection of p25α into OLN-t40-AS cells stably expressing α-syn caused degeneration as visualized by “rounding” of the cells in phase contrast microscopy and by retraction of the MT from the cellular processes to the perinuclear region as determined by immunofluorescence microscopy (Fig. 1A) (Kragh et al., 2009). When focusing on the approximately 40% of p25α expressing cells that display normal morphology (without MT retraction), we demonstrate significant higher nuclear translocation of NF-κB p65 in these apparent resilient cells compared to the “round” cells (with MT retraction) (30% *vs* 7% (Fig. 3A and B)). Control experiments with cells transfected with empty pcDNA3.1 vector yielded a diffuse distribution of NF-κB p65 in the cytoplasm with nuclear translocation in approximately 2% of the cells (Fig. 3A). Accordingly, the majority of p25α-expressing cells with nuclear NF-κB p65 staining did not demonstrate MT retraction (Fig. 3B) indicating that NF-κB activation serves a protective function against toxic α-syn species formed within the cells.

To investigate whether aggregation and Ser129-phosphorylation of α-syn is involved in stress that causes NF-κB p65 translocation in our model, we co-transfected OLN-93 cells with pcDNA3.1 expression vectors encoding α-syn wt or α-syn S129A in combination with p25α and used the cell permeable peptide ASI1D (El Agnaf et al., 2004) to inhibit aggregation of α-syn. Fig. 3C demonstrates that both removal of the Ser129 phosphorylation site and treatment with the ASI1D peptide significantly reduced NF-κB p65 translocation

and MT retraction compared to cells expressing α-syn wt and p25α. Hence, both IκBα mRNA induction and activation of NF-κB and thereby induction of resilience is downstream of both aggregation and Ser129 phosphorylation of α-syn.

To ascertain that NF-κB p65 translocation is associated with activation of NF-κB responsive genes we investigated the effect of α-syn toxicity on the induction of the proinflammatory cytokine, IL6, a well-described NF-κB target gene (Lee and Burckart, 1998). Co-expression of α-syn and p25α caused an upregulation of IL6 mRNA (Fig. 3D), thus validating the gene array data (Table 1) and indicating that nuclear NF-κB p65 translocation in oligodendroglial cells is followed by transcriptional induction of NF-κB target genes.

Increased expression of IκBα in hα-syn expressing oligodendrocytes in vivo

To validate the results obtained in the oligodendroglial OLN-93 cell line and assure α-syn expression induces IκBα expression *in vivo* we investigated two transgenic mouse lines expressing human α-syn under the oligodendrocyte specific MBP promoter. Lines MBP1 and MBP29 both display behavioral deficits after 3 months (Shults et al., 2005) whereas the live span of MBP1 is similar to ntg mice MBP29 suffers a more debilitating disease course and die within 6 months of age. Immunohistochemical analyses of 3 months old MBP-hα-syn mice (line 1 and 29) demonstrate astrogliosis and neuroinflammation, as detected using antibodies against GFAP (astrocytes) and Iba1 (activated microglia) in corpus callosum of MBP29 mice whereas MBP1 does not differ from ntg controls (Fig. 4D).

IκBα expression was analyzed by real-time quantitative PCR of total brain extracts from 3 months old ntg and MBP-hα-syn mice. The expression level of IκBα mRNA was significantly increased in both slowly degenerating MBP1 and fast degenerating MBP29 mice compared to ntg mice (Fig. 4A). Additionally, the level of IL6 mRNA was increased, further corroborating the results obtained in our oligodendrocyte cell line. Western blot analysis revealed a small, but significant, increase in IκBα protein levels in the soluble fraction of total brain extracts from MBP29 mice compared to ntg mice but no change in NF-κB p65 protein levels (Fig. 4B and C). Protein levels were not changed in MBP1 mice when compared to controls (data not shown).

To determine which cell types contribute to the increased IκBα expression in the 3 months old MBP29 mice double-labeling immunohistochemistry was conducted (Fig. 4E–G). The strong oligodendroglial expression of α-syn was evident by double-labeling studies of white matter in corpus callosum using antibodies against α-syn and the oligodendroglial marker p25α (Lindersson et al., 2005) (Fig. 4E) The oligodendrocytes were responsible for the majority of the IκBα expression in corpus callosum as demonstrated by colocalization of IκBα and p25α where most IκBα-positive cells co-expressed p25α (Fig. 4E). To determine if the tissue stress induced by oligodendroglial α-syn expression also caused IκBα expression in other cell types we conducted double labeling of IκBα with the astrocyte marker GFAP and the neuronal marker NeuN in neocortex. Astrocytes in ntg control mice did not express IκBα in contrast to the MBP29 mice where colocalization between GFAP and IκBα was observed in about 12–15% of the cell bodies (Fig. 4F). By contrast, some neurons in ntg mice express IκBα in a coarse granular pattern that colocalized with NeuN and this expression was increased in the MBP29 mice (Fig. 4G).

To corroborate these double labeling immunohistochemical analyses we conducted in situ hybridization (ISH) analysis of IκBα mRNA expression, combined with immunohistochemistry using antibodies to p25α, GFAP and NeuN as markers for oligodendrocytes, astrocytes and neurons (Fig. 4H). We demonstrate strong IκBα mRNA expression in oligodendrocytes in white matter of corpus callosum and in cortical neurons and lesser intense hybridization to astrocytes from MBP29 mice. Sections hybridized with the sense probe but not subjected to immunohistochemistry showed no signal (Fig. 4H).

Conclusively, increased IκBα mRNA is observed in both MBP1 and MBP29 mice but enhanced IκBα protein levels are only detected in brain homogenates by immunoblotting in the rapidly degenerating MBP29 line. In the reactive tissue of the MBP29 mice IκBα antigen is enhanced in oligodendrocytes, astrocytes and neurons.

Expression of NF-κB and IκBα proteins in human MSA brain tissue

α-Syn aggregates accumulate within p25α expressing oligodendrocytes in MSA so we investigated the expression levels of IκBα and NF-κB protein in the soluble fraction of post mortem human brain samples from MSA patients and control subjects similar to our approach for the MBP mice. The levels were quantified by immunoblotting for IκBα and NF-κB p65 proteins using actin as loading control. All MSA cases had typical clinical disease and an average duration from diagnosis (O'Sullivan et al., 2008). All had pathological GCIs, a pathognomonic increase in insoluble α-syn (Fig. 5A, Suppl. Fig. 1) and an unchanged level of soluble α-syn, consistent with previous literature (Tong et al., 2010).

The soluble 37 kDa IκBα from end-stage MSA tissue was significantly reduced compared to controls (0.54 fold) (Fig. 5B) and thus differed from the MSA mouse model. IκBα is a component of α-syn rich Lewy body inclusions (Noda et al., 2005) so we tested if the reduced level in the soluble MSA fraction could be due to a redistribution of soluble IκBα into the insoluble fraction that harbors the α-syn aggregates in MSA (Fig. 5A). Although the insoluble IκBα level may appear to be increased in Fig. 5A this was not significant due to the variations in protein loading and in the varying IκBα levels of the control group (Suppl Fig. 1).

The NF-κB p65 protein was also reduced in the soluble fraction (0.53 fold; Fig. 5C). The p65 protein activates the NF-κB system by translocating from the cytosol into the nucleus where it binds to DNA and thus change from being buffer soluble to insoluble. The insoluble fraction from MSA brain contained significantly more p65 protein than control (1.55 fold; Fig. 5D) and this change was more pronounced when presented as the ratio between insoluble and soluble NF-κB that increased more than 3-fold (Fig. 5E). The large variability in the ratio of insoluble/soluble NF-κB in MSA was not the result of a correlation with the accumulations of insoluble α-syn and IκBα proteins (Fig. 1 suppl). Thus, in tissue affected by MSA a shift occurs in the solubility of NF-κB p65 into insoluble fractions and this may be a functional consequence of the reduction in soluble IκBα that sequesters NF-κB in the cytotol.

To determine if MSA brain pathology is associated with changes in cellular IκBα and NF-κB p65 expression in oligodendrocytes, astrocytes and neurons we conducted immunohistochemistry of pontine white matter.

Evidently IκBα expression is sparse in control white matter tissue compared to the strong expression in MSA tissue (Fig. 6, A,vs B and C). The increased expression is to some extend accounted for by expression in oligodendrocytes carrying GCIs as demonstrated by the colocalization of α-syn and IκBα immunoreactivity (Fig. 6, B and C, arrows) with isolated GCIs containing significant IκBα immunoreactivity in association with IκBα immunopositive nuclei (Fig. 6, B, asterisk). However, the majority of the increased IκBα is located in reactive astrocytes (Fig. 6, B and C). The localization of IκBα in astrocytes was validated by double-labelling immunofluorescence using the astrocytic marker GFAP that demonstrated IκBα in the cell body and proximal processes (Fig. 6, E and F). Bright NF-κB p65 immunoreactivity was also accumulated in MSA astrocytes (Fig. 6, D)

Accumulation of p25α protein in the enlarged cell body of oligodendrocytes has been described as consistent and early characteristic of MSA (Song et al., 2007).. A proportion (13%) of the enlarged oligodendrocytes colocalized p25α and NF-κB p65 in the cytoplasmic inclusions (Fig. 6, G–J) that both resembled the early perinuclear deposits (Fig. 6, G–I) and the more mature GCI expanding the cell body away from the nucleus (Fig. 6, J). Approximately 4–6% had NF-κB in the nucleus (Fig. 6, I).

Double labeling of IκBα and NF-κB p65 in oligodendrocytes demonstrated a weakly stained cytoplasmic colocalization of the two antigens that was more abundant and intense in MSA (Fig. 6, K vs L) and confirmed the localization of NF-κB in the nucleus (see Fig. 6, I) of some (4–6%) oligodendrocytes where it colocalized with IκBα immunoreactivity throughout the nucleus (Fig. 6, N–O). Like in mice, human neurons from control tissue express IκBα but it does not colocalize with NF-κB p65 (Fig. 6, M).

In conclusion, the immunohistological analyses of human MSA tissue demonstrate a large complexity in the tissue elements expressing IκBα protein with reactive astrocytes as prominent contributors in pontine white matter. This may well be subject to local variation based on degree of GCI accumulation, neurodegeneration, astrogliosis and neuroinflammation.

Discussion

We have previously developed a cell model of MSA based on the coexpression of the oligodendroglial p25α protein with α-syn in rat oligodendroglial OLN-93 cell lines (Kragh et al., 2009). In this model of α-syn aggregation- and Ser129-phosphorylation-dependent degeneration we investigated if the NF-κB stress response system plays regulatory roles in determining the degenerative phenotype and discovered two functionally opposing actions; activation of cytoprotective NF-κB signaling that is counteracted by expression of its prodegenerative inhibitor IκBα.

OLN-93 cells coexpressing α-syn and p25α displayed two different phenotypes; a degenerative phenotype where cells undergo fast MT retraction and a resilient phenotype

indistinguishable from the non-transfected cells. The resilient cells displayed almost four times higher activation of NF-κB as determined by nuclear p65 translocation indicating a protective effect of NF-κB activation. This was corroborated by use of the NF-κB inhibitor NBD-peptide that induced an almost complete loss of the resilient phenotype. Interestingly, we demonstrate that approximately 13% of MSA oligodendrocytes have detectable NF-κB colocalized with p25α in their GCIs in contrast to a smaller fraction of 4–6% where NF-κB was in the nucleus and these cellular phenotypes could thus hypothetically represent actively degenerating and resistant cells or early and later steps in the degenerative process. Similar protective cell autonomous NF-κB functions have been demonstrated in oligodendroglial cells subjected to stress from TNF-α, IFN-γ, unfolded proteins and reactive oxygen and nitrogen species (Hamanoue et al., 2004; Lin et al., 2012). In this respect, oligodendrocytes may resemble glutamatergic forebrain neurons where NF-κB signaling protects against oxidative and excitotoxic stress (Fridmacher et al., 2003). A link between pathological oligodendroglial α-syn expression and protective NF-κB activation has been suggested in multiple sclerosis where oligodendrocytes express α-syn around active demyelinating lesions (Lu et al., 2009) and NF-κB activation is protective for the oligodendrocytes (Bonetti et al., 1999).

The magnitude of IκBα expression during α-syn aggregate stress likely represents the switch determining the cellular outcome of degeneration versus resilience. The strongest evidence for this hypothesis is the protective effect and concomitant nuclear NF-κB translocation induced by lowering IκBα mRNA by siRNA. Moreover, the stress that upregulated IκBα mRNA required both aggregation and Ser129-phosphorylation of α-syn, which are prerequisites for the stress inducing degeneration in this model (Kragh et al., 2009).

Mechanisms causing the accumulation of IκBα mRNA are still unclear. IκBα mRNA is stabilized by heat shock wherein protein misfolding plays a prominent role and thus may resemble the induction of misfolded α-syn in our model (Dunsmore et al., 2006; Malhotra et al., 2002; Wong et al., 1997). Alternatively, IκBα mRNA expression could represent an exaggerated response to an initial beneficial NF-κB activation because IκBα can act as a negative feedback loop induced by NF-κB activation (Chiao et al., 1994). The increased IκBα protein in our MSA mouse model could also represent a response to oxidative stress that has been demonstrated to inhibit the ubiquitination of phosphorylated IκBα otherwise destined for degradation (Kalita et al., 2011; Narayan et al., 2012). Irrespective of mechanism, our results suggest the strong reduction of NF-κB activation in α-syn expressing SH-SY5Y cells could be the result of an increased IκBα expression (Yuan et al., 2008).

MSA represents a fast progressing neurodegenerative disorder characterized by a complex tissue remodeling involving oligodendroglial degeneration, axonal and neuronal loss, astrogliosis and neuroinflammation with microglia accumulation and activation (Halliday et al., 2011; Song et al., 2007; Ubhi et al., 2011; Wenning et al., 2008). This makes it difficult to elucidate whether a degenerative cell autonomous oligodendroglial IκBα response occurs in human MSA tissue. The disease-defining hallmark is the oligodendrocytic accumulation of aggregated α-syn in GCIs and the cytopathology evolves in stages during the differentiation of oligodendroglia precursor cells to end-stage shrunken and GCI-containing

oligodendrocytes (Kragh et al., 2013; Song et al., 2007). This process may involve decisive steps that can represent therapeutic targets because we identified IκBα expression early in our cell model where no morphological phenotype was detectable. In end-stage MSA brain tissue, we demonstrate that astrocytes exhibit the strongest IκBα staining although expression also occurs in α-syn expressing oligodendrocytes. The astrocytic IκBα response could represent a protective response because stabilizing astrocytic IκBα by cell specific IκB kinase 2 depletion protects oligodendrocytes in a toxic model of demyelination (Raasch et al., 2011).

To circumvent the complexity of human MSA tissue we used two transgenic mouse lines, MBP-ha-syn lines 1 and 29, which express human α-syn in oligodendrocytes (Shults et al., 2005). The MBP promoter assures that expression is initiated from the stage of myelination and does not affects oligodendroglial precursor cells. The phenotype of the two lines are strikingly different with line 29 expressing high levels of α-syn, strong tissue activation with neurodegeneration and ultimately death within 6 months whereas the intermediate-expressing line 1 demonstrates minimal tissue response, no increased mortality within 18 months but an early onset motor behavioral phenotype. We investigated these lines at 3 months of age when line 1 did not display any detectable astrocytic and neuroinflammatory response in contrast to line 29.

We demonstrate that IκBα is constitutively expressed in neurons of mouse and human brain and this makes it more difficult to evaluate the IκBα expression data in the MBP mouse model. However, we are able to demonstrate increased mRNA expression in various brain regions of both line 1 and 29 and also increased IκBα protein in 3 months old MBP29 mice. The IκBα protein was almost completely colocalized with the oligodendroglial marker p25α in the white matter structure corpus callosum of 3 months old line 29 mice although increased expression also was noted in reactive astrocytes in tissue displaying neuroinflammation and astrogliosis. This contrasts human MSA tissue that displays the strongest IκBα expression in reactive astrocytes and may reflect that MBP mice allow modeling of early phases of MSA pathophysiology. Despite the complex tissue response, the α-syn-dependent IκBα expression observed in the cell model mirror the response in α-syn expressing oligodendrocytes in intact brain and thus corroborates the hypothesis that IκBα serves a prodegenerative function.

NF-κB signaling has predominantly been considered as a detrimental factor in many diseases because it often contributes to tissue inflammatory processes where proinflammatory cytokines are transcribed that modulate tissue and organismal responses (Lawrence, 2009). However, NF-κB activation also serves physiological functions as demonstrated in neurons and brain (Boersma and Meffert, 2008; Kaltschmidt and Kaltschmidt, 2009) and cytoprotective functions, which can pose a problem in cancer therapy (Xiao and Fu, 2011). The functional outcome of NF-κB inducing stress rely on the mode of activation as exemplified by the plasma membrane death domain receptors FAS and TNF-R that can trigger both apoptotic and protective pathways in response to NF-κB activation (Imamura et al., 2004). SIRT2 dependent deacetylation of RIP-1 kinase changes TNF-R signaling from an activator of protective NF-κB signaling to an inducer of necrosis (Narayan et al., 2012). SIRT2 inhibition is neuroprotective in some PD models (Outeiro et

al., 2007) and α-syn aggregate-dependent sensitization to SIRT2 activity could play a functional role in oligodendroglial MSA models where FAS dependent signaling is turned into a cytotoxic path (Kragh et al., 2013). Small molecule NF-κB activators have recently been identified that presumably stabilize p65 binding to its DNA response elements (Manuvakhova et al., 2011) and may be tested for protective efficacy in disease settings with decreased NF-κB activation, e.g. due to SIRT2 activation (de Oliveira et al., 2012).

NF-κB activation is mediated by translocation of p65 and p50 transcription factors from the cytosol into the nucleus. This translocation results in a fundamental change in p65 solubility in simple tissue homogenates that may be the reason for the 3-fold increased ratio of insoluble to soluble p65 in the precentral gyrus white matter. The biochemical data suggest that there is an activation of NF-κB in MSA white matter. Although its cellular origin is still unknown our demonstration of nuclear NF-κB in approximately 5% of MSA oligodendrocytes suggest it could reflect a protective response. This may be tested by investigating p65 solubility and oligodendroglial nuclear localization in MSA tissue sampled from brain regions of active neurodegeneration versus more resilient regions, e.g. pontine white matter tracts and forebrain cortex, and compare these changes to the temporal changes in NF-κB activation in MSA mouse models. The outcome of such investigations will guide the identification of time intervals where pharmacological stabilization of nuclear p65 may be appropriate because general long-term NF-κB activation is likely to cause destructive neuroinflammatory tissue responses.

Conclusively, our data suggest cell-autonomous NF-κB inhibition in oligodendrocytes by IκBα represents a prodegenerative mechanism in MSA pathophysiology down-stream of α-syn accumulation. Although human MSA tissue shows evidence of generalized NF-κB activation that likely represents neuroinflammation, selective stabilization of oligodendroglial NF-κB activation or down-stream signaling pathways represent potential targets for inducing resilience to MSA related oligodendroglial degeneration.

Supplementary Material

Refer to Web version on PubMed Central for supplementary material.

References

Boersma MC, Meffert MK. Novel roles for the NF-kappaB signaling pathway in regulating neuronal function. Science signaling. 2008; 1:pe7. [PubMed: 18272467]

Bonetti B, Stegagno C, Cannella B, Rizzuto N, Moretto G, Raine CS. Activation of NF-kappaB and c-jun transcription factors in multiple sclerosis lesions. Implications for oligodendrocyte pathology. Am J Pathol. 1999; 155:1433–1438. [PubMed: 10550297]

Burn DJ, Jaros E. Multiple system atrophy: cellular and molecular pathology 6. Journal of Clinical Pathology-Molecular Pathology. 2001; 54:419–426.

Chiao PJ, Miyamoto S, Verma IM. Autoregulation of I kappa B alpha activity. Proc Natl Acad Sci U S A. 1994; 91:28–32. [PubMed: 8278379]

de Oliveira RM, Sarkander J, Kazantsev AG, Outeiro TF. SIRT2 as a Therapeutic Target for Age-Related Disorders. Frontiers in pharmacology. 2012; 3:82. [PubMed: 22563317]

Dickson DW, Lin WL, Liu WK, Yen SH. Multiple system atrophy: A sporadic synucleinopathy. Brain Pathology. 1999; 9:721–732. [PubMed: 10517510]

Dunsmore KE, Denenberg AG, Page K, Wong HR. Mechanism and function of heat shock-dependent IkappaBalpha expression. Inflamm Res. 2006; 55:254–259. [PubMed: 16955245]

El Agnaf OMA, Paleologou KE, Greer B, Abogrein AM, King JE, Salem SA, Fullwood NJ, Benson FE, Hewitt R, Ford KJ, Martin FL, Harriot P, Cookson MR, Allsop D. A strategy for designing inhibitors of alpha-synuclein aggregation and toxicity as a novel treatment for Parkinson's disease and related disorders 2. Faseb Journal. 2004; 18:1315-+. [PubMed: 15180968]

Farrer M, Kachergus J, Forno L, Lincoln S, Wang DS, Hulihan M, Maraganore D, Gwinn-Hardy K, Wszolek Z, Dickson D, Langston JW. Comparison of kindreds with parkinsonism and alpha-synuclein genomic multiplications 10. Annals of Neurology. 2004; 55:174–179. [PubMed: 14755720]

Fridmacher V, Kaltschmidt B, Goudeau B, Ndiaye D, Rossi FM, Pfeiffer J, Kaltschmidt C, Israel A, Memet S. Forebrain-specific neuronal inhibition of nuclear factor-kappaB activity leads to loss of neuroprotection. J Neurosci. 2003; 23:9403–9408. [PubMed: 14561868]

Gai WP, Power JH, Blumbergs PC, Culvenor JG, Jensen PH. Alpha-synuclein immunoisolation of glial inclusions from multiple system atrophy brain tissue reveals multiprotein components. J. Neurochem. 1999; 73:2093–2100. [PubMed: 10537069]

Ghosh A, Roy A, Liu X, Kordower JH, Mufson EJ, Hartley DM, Ghosh S, Mosley RL, Gendelman HE, Pahan K. Selective inhibition of NF-kappaB activation prevents dopaminergic neuronal loss in a mouse model of Parkinson's disease. Proc Natl Acad Sci U S A. 2007; 104:18754–18759. [PubMed: 18000063]

Halliday GM, Holton JL, Revesz T, Dickson DW. Neuropathology underlying clinical variability in patients with synucleinopathies. Acta Neuropathol. 2011; 122:187–204. [PubMed: 21720849]

Hamanoue M, Yoshioka A, Ohashi T, Eto Y, Takamatsu K. NF-kappaB prevents TNF-alpha-induced apoptosis in an oligodendrocyte cell line. Neurochem Res. 2004; 29:1571–1576. [PubMed: 15260136]

Hunot S, Brugg B, Ricard D, Michel PP, Muriel MP, Ruberg M, Faucheux BA, Agid Y, Hirsch EC. Nuclear translocation of NF-kappaB is increased in dopaminergic neurons of patients with parkinson disease. Proc Natl Acad Sci U S A. 1997; 94:7531–7536. [PubMed: 9207126]

Imamura R, Konaka K, Matsumoto N, Hasegawa M, Fukui M, Mukaida N, Kinoshita T, Suda T. Fas ligand induces cell-autonomous NF-kappaB activation and interleukin-8 production by a mechanism distinct from that of tumor necrosis factor-alpha. J Biol Chem. 2004; 279:46415–46423. [PubMed: 15337758]

Jellinger KA. Neuropathological spectrum of synucleinopathies 6. Movement Disorders. 2003; 18:S2–S12. [PubMed: 14502650]

Kahle PJ, Neumann M, Ozmen L, Muller V, Jacobsen H, Spooren W, Fuss B, Mallon B, Macklin WB, Fujiwara H, Hasegawa M, Iwatsubo T, Kretzschmar HA, Haass C. Hyperphosphorylation and insolubility of alpha-synuclein in transgenic mouse oligodendrocytes. Embo Reports. 2002; 3:583–588. [PubMed: 12034752]

Kalita MK, Sargsyan K, Tian B, Paulucci-Holthauzen A, Najm HN, Debusschere BJ, Brasier AR. Sources of cell-to-cell variability in canonical nuclear factor-kappaB (NF-kappaB) signaling pathway inferred from single cell dynamic images. The Journal of biological chemistry. 2011; 286:37741–37757. [PubMed: 21868381]

Kaltschmidt B, Kaltschmidt C. NF-kappaB in the nervous system. Cold Spring Harb Perspect Biol. 2009; 1:a001271. [PubMed: 20066105]

Kiely AP, Asi YT, Kara E, Limousin P, Ling H, Lewis P, Proukakis C, Quinn N, Lees AJ, Hardy J, Revesz T, Houlden H, Holton JL. alpha-Synucleinopathy associated with G51D SNCA mutation: a link between Parkinson's disease and multiple system atrophy? Acta neuropathologica. 2013; 125:753–769. [PubMed: 23404372]

Kragh CL, Lund LB, Febbraro F, Hansen HD, Gai WP, El-Agnaf O, Richter-Landsberg C, Jensen PH. {alpha}-Synuclein Aggregation and Ser-129 Phosphorylation-dependent Cell Death in Oligodendroglial Cells. J Biol Chem. 2009; 284:10211–10222. [PubMed: 19203998]

Kragh CL, Fillon G, Gysbers A, Hansen HD, Neumann M, Richter-Landsberg C, Haass C, Zalc B, Lubetzki C, Gai WP, Halliday GM, Kahle PJ, Jensen PH. FAS-dependent cell death in alpha-

synuclein transgenic oligodendrocyte models of multiple system atrophy. PLoS One. 2013; 8:e55243. [PubMed: 23372841]

Kruger R, Eberhardt O, Riess O, Schulz JB. Parkinson's disease: one biochemical pathway to fit all genes? Trends Mol. Med. 2002; 8:236–240. [PubMed: 12067634]

Lawrence T. The nuclear factor NF-kappaB pathway in inflammation. Cold Spring Harb Perspect Biol. 2009; 1:a001651. [PubMed: 20457564]

Lee JI, Burckart GJ. Nuclear factor kappa B: important transcription factor and therapeutic target. J Clin Pharmacol. 1998; 38:981–993. [PubMed: 9824778]

Lenardo MJ, Baltimore D. NF-kappa B: a pleiotropic mediator of inducible and tissue-specific gene control. Cell. 1989; 58:227–229. [PubMed: 2665943]

Lin Y, Jamison S, Lin W. Interferon-gamma activates nuclear factor-kappa B in oligodendrocytes through a process mediated by the unfolded protein response. PLoS One. 2012; 7:e36408. [PubMed: 22574154]

Lindersson E, Lundvig D, Petersen C, Madsen P, Nyengaard JR, Hojrup P, Moos T, Otzen D, Gai WP, Blumbergs PC, Jensen PH. p25alpha Stimulates alpha-synuclein aggregation and is co-localized with aggregated alpha-synuclein in alpha-synucleinopathies. J. Biol. Chem. 2005; 280:5703–5715. [PubMed: 15590652]

Lu JQ, Fan Y, Mitha AP, Bell R, Metz L, Moore GR, Yong VW. Association of alpha-synuclein immunoreactivity with inflammatory activity in multiple sclerosis lesions. J Neuropathol Exp Neurol. 2009; 68:179–189. [PubMed: 19151622]

Malhotra V, Eaves-Pyles T, Odoms K, Quaid G, Shanley TP, Wong HR. Heat shock inhibits activation of NF-kappaB in the absence of heat shock factor-1. Biochem Biophys Res Commun. 2002; 291:453–457. [PubMed: 11855810]

Manuvakhova MS, Johnson GG, White MC, Ananthan S, Sosa M, Maddox C, McKellip S, Rasmussen L, Wennerberg K, Hobrath JV, White EL, Maddry JA, Grimaldi M. Identification of novel small molecule activators of nuclear factor-kappaB with neuroprotective action via high-throughput screening. J Neurosci Res. 2011; 89:58–72. [PubMed: 21046675]

Narayan N, Lee IH, Borenstein R, Sun J, Wong R, Tong G, Fergusson MM, Liu J, Rovira II, Cheng HL, Wang G, Gucek M, Lombard D, Alt FW, Sack MN, Murphy E, Cao L, Finkel T. The NAD-dependent deacetylase SIRT2 is required for programmed necrosis. Nature. 2012; 492:199–204. [PubMed: 23201684]

Noda K, Kitami T, Gai WP, Chegini F, Jensen PH, Fujimura T, Murayama K, Tanaka K, Mizuno Y, Hattori N. Phosphorylated IkappaBalpha is a component of Lewy body of Parkinson's disease. Biochem Biophys Res Commun. 2005; 331:309–317. [PubMed: 15845394]

O'Sullivan SS, Massey LA, Williams DR, Silveira-Moriyama L, Kempster PA, Holton JL, Revesz T, Lees AJ. Clinical outcomes of progressive supranuclear palsy and multiple system atrophy. Brain : a journal of neurology. 2008; 131:1362–1372. [PubMed: 18385183]

Outeiro TF, Kontopoulos E, Altmann SM, Kufareva I, Strathearn KE, Amore AM, Volk CB, Maxwell MM, Rochet JC, McLean PJ, Young AB, Abagyan R, Feany MB, Hyman BT, Kazantsev AG. Sirtuin 2 inhibitors rescue alpha-synuclein-mediated toxicity in models of Parkinson's disease 1. Science. 2007; 317:516–519. [PubMed: 17588900]

Papa S, Zazzeroni F, Pham CG, Bubici C, Franzoso G. Linking JNK signaling to NF-kappaB: a key to survival. J. Cell Sci. 2004; 117:5197–5208. [PubMed: 15483317]

Papp MI, Kahn JE, Lantos PL. Glial cytoplasmic inclusions in the CNS of patients with multiple system atrophy (striatonigral degeneration, olivopontocerebellar atrophy and Shy-Drager syndrome). Journal of the neurological sciences. 1989; 94:79–100. [PubMed: 2559165]

Polymeropoulos MH, Lavedan C, Leroy E, Ide SE, Dehejia A, Dutra A, Pike B, Root H, Rubenstein J, Boyer R, Stenroos ES, Chandrasekharappa S, Athanassiadou A, Papapetropoulos T, Johnson WG, Lazzarini AM, Duvoisin RC, Di Iorio G, Golbe LI, Nussbaum RL. Mutation in the alpha-synuclein gene identified in families with Parkinson's disease. Science. 1997; 276:2045–2047. [PubMed: 9197268]

Richter-Landsberg C, Heinrich M. OLN-93: a new permanent oligodendroglia cell line derived from primary rat brain glial cultures 1. J. Neurosci. Res. 1996; 45:161–173. [PubMed: 8843033]

Raasch J, Zeller N, van Loo G, Merkler D, Mildner A, Erny D, Knobeloch KP, Bethea JR, Waisman A, Knust M, Del Turco D, Deller T, Blank T, Priller J, Bruck W, Pasparakis M, Prinz M. IkappaB kinase 2 determines oligodendrocyte loss by non-cell-autonomous activation of NF-kappaB in the central nervous system. Brain. 2011; 134:1184–1198. [PubMed: 21310728]

Shults CW, Rockenstein E, Crews L, Adame A, Mante M, Larrea G, Hashimoto M, Song D, Iwatsubo T, Tsuboi K, Masliah E. Neurological and neurodegenerative alterations in a transgenic mouse model expressing human alpha-synuclein under oligodendrocyte promoter: implications for multiple system atrophy. J. Neurosci. 2005; 25:10689–10699. [PubMed: 16291942]

Singleton AB, Farrer M, Johnson J, Singleton A, Hague S, Kachergus J, Hulihan M, Peuralinna T, Dutra A, Nussbaum R, Lincoln S, Crawley A, Hanson M, Maraganore D, Adler C, Cookson MR, Muenter M, Baptista M, Miller D, Blancato J, Hardy J, Gwinn-Hardy K. alpha-synuclein locus triplication causes Parkinson's disease. Science. 2003; 302:841–841. [PubMed: 14593171]

Song YJ, Lundvig DM, Huang Y, Gai WP, Blumbergs PC, Hojrup P, Otzen D, Halliday GM, Jensen PH. p25alpha relocalizes in oligodendroglia from myelin to cytoplasmic inclusions in multiple system atrophy. Am. J. Pathol. 2007; 171:1291–1303. [PubMed: 17823288]

Soos J, Engelhardt JI, Siklos L, Havas L, Majtenyi K. The expression of PARP, NF-kappa B and parvalbumin is increased in Parkinson disease. Neuroreport. 2004; 15:1715–1718. [PubMed: 15257133]

Togo T, Iseki E, Marui W, Akiyama H, Ueda K, Kosaka K. Glial involvement in the degeneration process of Lewy body-bearing neurons and the degradation process of Lewy bodies in brains of dementia with Lewy bodies. J Neurol Sci. 2001; 184:71–75. [PubMed: 11231035]

Tong J, Wong H, Guttman M, Ang LC, Forno LS, Shimadzu M, Rajput AH, Muenter MD, Kish SJ, Hornykiewicz O, Furukawa Y. Brain alpha-synuclein accumulation in multiple system atrophy, Parkinson's disease and progressive supranuclear palsy: a comparative investigation. Brain : a journal of neurology. 2010; 133:172–188. [PubMed: 19903734]

Ubhi K, Low P, Masliah E. Multiple system atrophy: a clinical and neuropathological perspective. Trends Neurosci. 2011; 34:581–590. [PubMed: 21962754]

Wakabayashi K, Hayashi S, Kakita A, Yamada M, Toyoshima Y, Yoshimoto M, Takahashi H. Accumulation of alpha-synuclein/NACP is a cytopathological feature common to Lewy body disease and multiple system atrophy. Acta Neuropathol.(Berl). 1998; 96:445–452. [PubMed: 9829807]

Wakabayashi K, Takahashi H. Cellular pathology in multiple system atrophy 1. Neuropathology. 2006; 26:338–345. [PubMed: 16961071]

Wenning GK, Stefanova N, Jellinger KA, Poewe W, Schlossmacher MG. Multiple system atrophy: a primary oligodendrogliopathy. Ann Neurol. 2008; 64:239–246. [PubMed: 18825660]

Wong HR, Ryan M, Wispe JR. Stress response decreases NF-kappaB nuclear translocation and increases I-kappaBalpha expression in A549 cells. J Clin Invest. 1997; 99:2423–2428. [PubMed: 9153285]

Xiao G, Fu J. NF-kappaB and cancer: a paradigm of Yin-Yang. American journal of cancer research. 2011; 1:192–221. [PubMed: 21969033]

Yazawa I, Giasson BI, Sasaki R, Zhang B, Joyce S, Uryu K, Trojanowski JQ, Lee VMY. Mouse model of multiple system atrophy alpha-synuclein expression in oligodendrocytes causes glial and neuronal degeneration 4. Neuron. 2005; 45:847–859. [PubMed: 15797547]

Yoshida M. Multiple system atrophy: alpha-synuclein and neuronal degeneration. Neuropathology. 2007; 27:484–493. [PubMed: 18018485]

Yuan Y, Jin J, Yang B, Zhang W, Hu J, Zhang Y, Chen NH. Overexpressed alpha-synuclein regulated the nuclear factor-kappaB signal pathway. Cell Mol Neurobiol. 2008; 28:21–33. [PubMed: 17712623]

Zarranz JJ, Alegre J, Gomez-Esteban JC, Lezcano E, Ros R, Ampuero I, Vidal L, Hoenicka J, Rodriguez O, Atares B, Llorens V, Tortosa EG, del Ser T, Munoz DG, de Yebenes JG. The new mutation, E46K, of alpha-synuclein causes Parkinson and Lewy body dementia 4. Annals of Neurology. 2004; 55:164–173. [PubMed: 14755719]

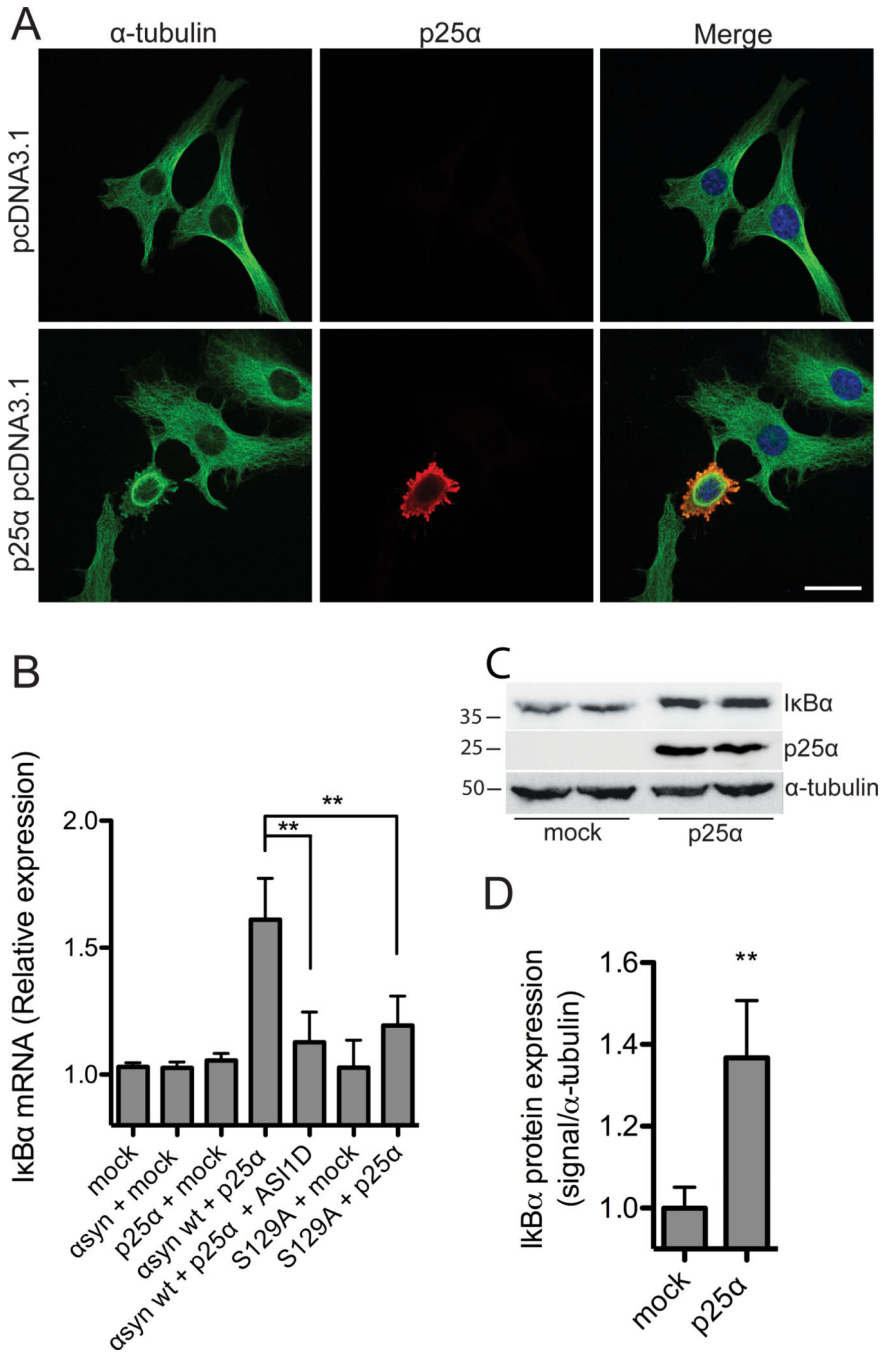

Figure 1. α-Synuclein dependent toxicity elicits IκBα expression

A, α-syn-expressing OLN-t40-AS cells were transiently transfected with an empty vector or p25α for 24 h and subjected to immunofluorescence microscopy using antibodies against α-tubulin (green) and p25α (red). Coexpression of α-syn and p25α causes retraction of the microtubule to the perinuclear region. Scale bar, 20 μm. B, OLN-wt cells were transiently transfected with α-syn wt or α-syn S129A in combination with p25α or empty vector for 24 h and treated with α-syn aggregate inhibitor peptide ASI1D as indicated. Total RNA was extracted and IκBα mRNA levels were analyzed by real-time qPCR. Fold changes were

determined from triplicate measurements and normalized to the NADH gene. Bars represent mean ± S.D. from three independent experiments. IκBα mRNA expression is significantly increased in cells coexpressing α-syn and p25α. This level of expression is reduced in cells treated with ASI1D and in cells expressing S129A (**$p < 0.01$) in which the level does not differ from control cells expressing solely p25α. C, OLN-t40-AS cells were transfected with empty vector or p25α for 24 h and cellular IκBα protein levels were detected by Western blotting. α-Tubulin was included as a loading control. D, Quantification of Western blot shown in C. IκBα protein is increased in OLN-t40-AS cells expressing p25α compared to cells expressing empty vector. Bars represent mean ± SD of three independent experiments. Asterisk demonstrates difference from mock ($p < 0.05$).

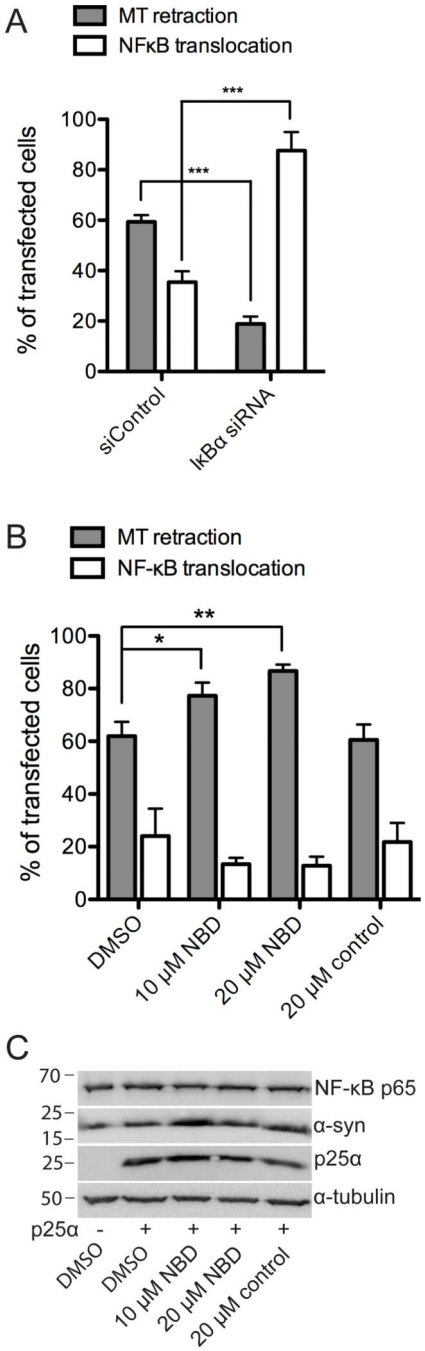

Figure 2. Inhibition of IκBα expression attenuates α-Synuclein-induced toxicity

A, OLN-t40-AS cells were transfected with a siRNA pool targeting rat IκBα mRNA and a non-targeting siControl pool for 72 h. Silencing efficiency after 72 h was 94% as confirmed by real-time qPCR. Following siRNA transfection, OLN-t40-AS cells were transfected with p25α for 24 h and the number of cells with MT retraction (grey bars) and nuclear translocation of the NF-κB transcription factor p65 (white bar) was quantified by immunofluorescence microscopy using antibodies against p25α, α-tubulin and NF-κB p65. RNAi-mediated silencing of IκBα expression caused a significant reduction in the number

of MT retracted degenerating cells (***$p < 0.001$) and a significant increase in nuclear NF-κB p65 staining (***$p < 0.001$). Bars represent mean ± S.D. from three independent experiments. B, OLN-t40-AS cells were transfected with p25α for 24 h and treated with NF-κB inhibitory cell permeable NBD peptide that stabilizes IκBα against degradation and control peptide when indicated. Cells were subjected to immunofluorescence microscopy using antibodies against p25α, α-tubulin and NF-κB p65 and quantified for MT retraction and NF-κB translocation. Bars represent mean ± S.D. from three independent experiments. Treatment with NBD peptide increases MT retraction in a dose-dependent manner (*$p < 0.05$, **$p < 0.01$). C, Western blot of whole cell extracts (30 μg protein) from transfected OLN-t40-AS cells was probed with antibodies against NF-κB p65, α-syn, and p25α. α-tubulin was included as loading control.

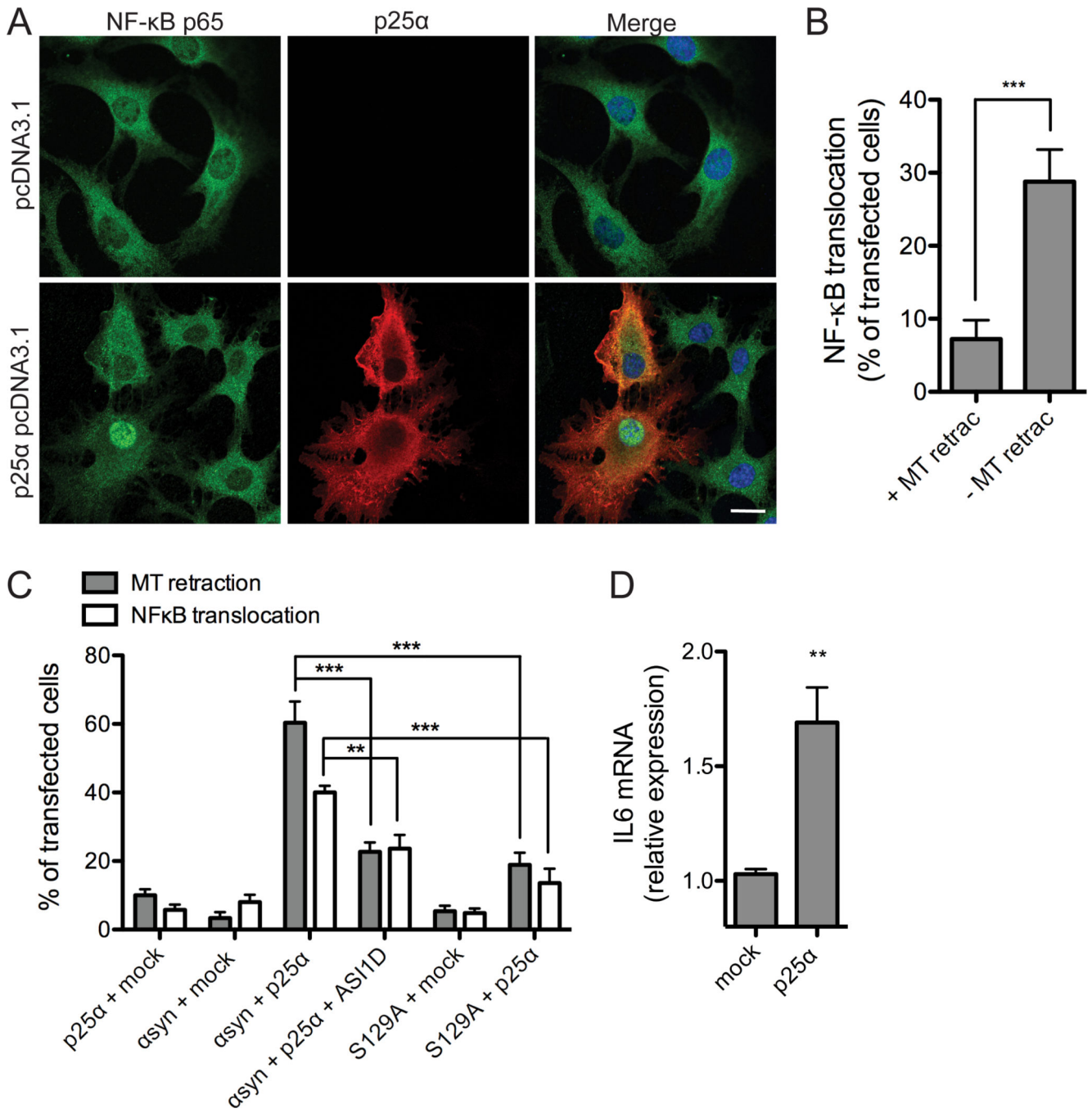

Figure 3. NF-κB activation accompanies α-synuclein dependent toxicity

A, α-syn-expressing OLN-t40-AS cells were transiently transfected with an empty vector or p25α for 24 h and subjected to immunofluorescence microscopy using antibodies against NF-κB p65 (green) and p25α (red). Co-expression of α-syn and p25α causes NF-κB p65 translocation from the cytoplasm to the nucleus in a fraction of p25α expressing cells. Scale bar, 20 μm. B, NF-κB translocation was quantified in OLN-t40-AS cells transfected with p25α, which demonstrated normal flat (− MT retraction) or round (+ MT retraction) morphology. Bars represent mean ± S.D. from three independent experiments. The nuclear

translocation of NF-κB p65 was significant higher in cells without MT retraction compared to “round” cells (with MT retraction) (***$p < 0.001$). C, Nuclear localization of NF-κB p65 was quantified in OLN-93 cells transiently expressing α-syn wt or α-syn S129A in combination with p25α or empty vector. Cells were treated with α-syn aggregation inhibitor peptide ASI1D when indicated. Bars represent mean ± S.D. from three independent experiments. NF-κB is translocated to the nucleus in response to coexpression of α-syn and p25α. Treatment with ASI1D peptide or coexpressing S129A with p25α significantly reduces the number of cells with MT retraction and nuclear NF-κB staining compared to coexpression of p25α and α-syn wt (**$p < 0.01$, ***$p < 0.001$). D, To investigate NF-κB responsive gene expression, IL6 mRNA levels were analyzed by real-time qPCR in OLN-t40-AS cells transiently transfected with p25α or empty vector for 24 h. Fold changes were determined from triplicate measurements and normalized to the NADH gene. Bars represent mean ± S.D. from three independent experiments. IL6 mRNA expression is increased 1.7-fold in cells coexpressing α-syn and p25α ($p < 0.05$).

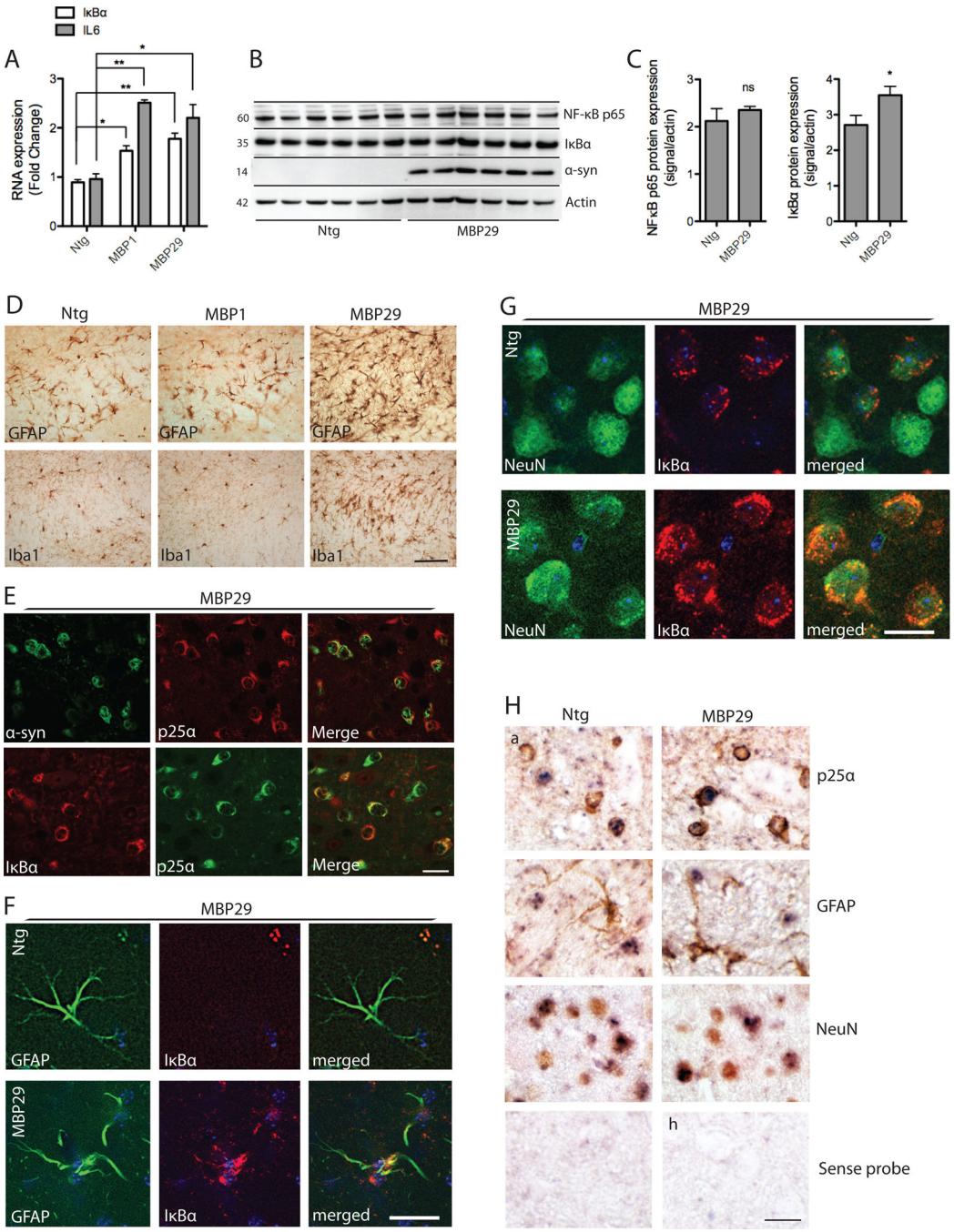

Figure 4. IκBα expression in MBP-hα-syn transgenic mice

A, IκBα and IL6 mRNA from total brain extracts of MBP-hα-syn tg (line 1 and 29) and ntg mice (n=6; age=3 months) were analyzed by real-time qPCR. Fold changes were determined from triplicate measurements and normalized to mouse GAPDH. Bars represent mean ± S.D. from three independent experiments. IκBα and IL6 mRNA are significantly increased in both line 1 and 29 as compared to ntg mice (*$p < 0.05$, **$p < 0.01$). B, IκBα and NF-κB p65 protein levels in line 29 mouse brain homogenates were analyzed by western blot analysis. β-actin is included as a loading control. Representative blots from n=6 of each

group are shown. C, Quantitative analysis of the levels of IκBα and NF-κB p65 demonstrates a significant increase in IκBα expression in tg mice compared to ntg controls (*$p < 0.05$) whereas there was no difference in NF-κB p65 levels between groups. D, Immunohistochemical analysis of corpus callosum with antibodies against GFAP and Iba1 shows that MBP-hα-syn line 29 (3 months old) displays severe astrogliosis and microgliosis in corpus callosum as compared to a ntg control (a,d). There was no difference in the expression of these proteins between the intermediate-expresser line 1 and the ntg control. Scale bar, 50 μm. E, Double labeling immunofluorescence microscopy of corpus callosum reveals colocalization of α-syn (green) and p25α (red) and of IκBα (red) and p25α (green) in corpus callosum of 3 months old line 29 mice. Scale bar, 30 μm. F–G, Double labeling studies for IκBα in neocortex of line 29 mice. Sections were double labeled with antibodies against the astroglial marker GFAP (F) and the neuronal marker NeuN (G) and IκBα. Scale bar, 10 μm. F, There was IκBα immunostaining of astrocytes in line 29 mice compared to ntg controls. G, In ntg mice occasional IκBα immunoreactivity was observed. In the MBP-α-syn tg mice there was an increase in IκBα immunolabeling. H, To validate the cell type-specific IκBα mRNA expression, *in situ* hybridization with a probe against IκBα (blue) and co-immunolabeling with markers for oligodendrocytes (p25α) and astroglial (GFAP) in corpus callosum, and neuronal (NeuN) antibodies (brown) in neocortex was conducted in 3 months old ntg and line 29 mice. *In situ* hybridization with sense probe showed no signal. Scale bar, 30 μm.

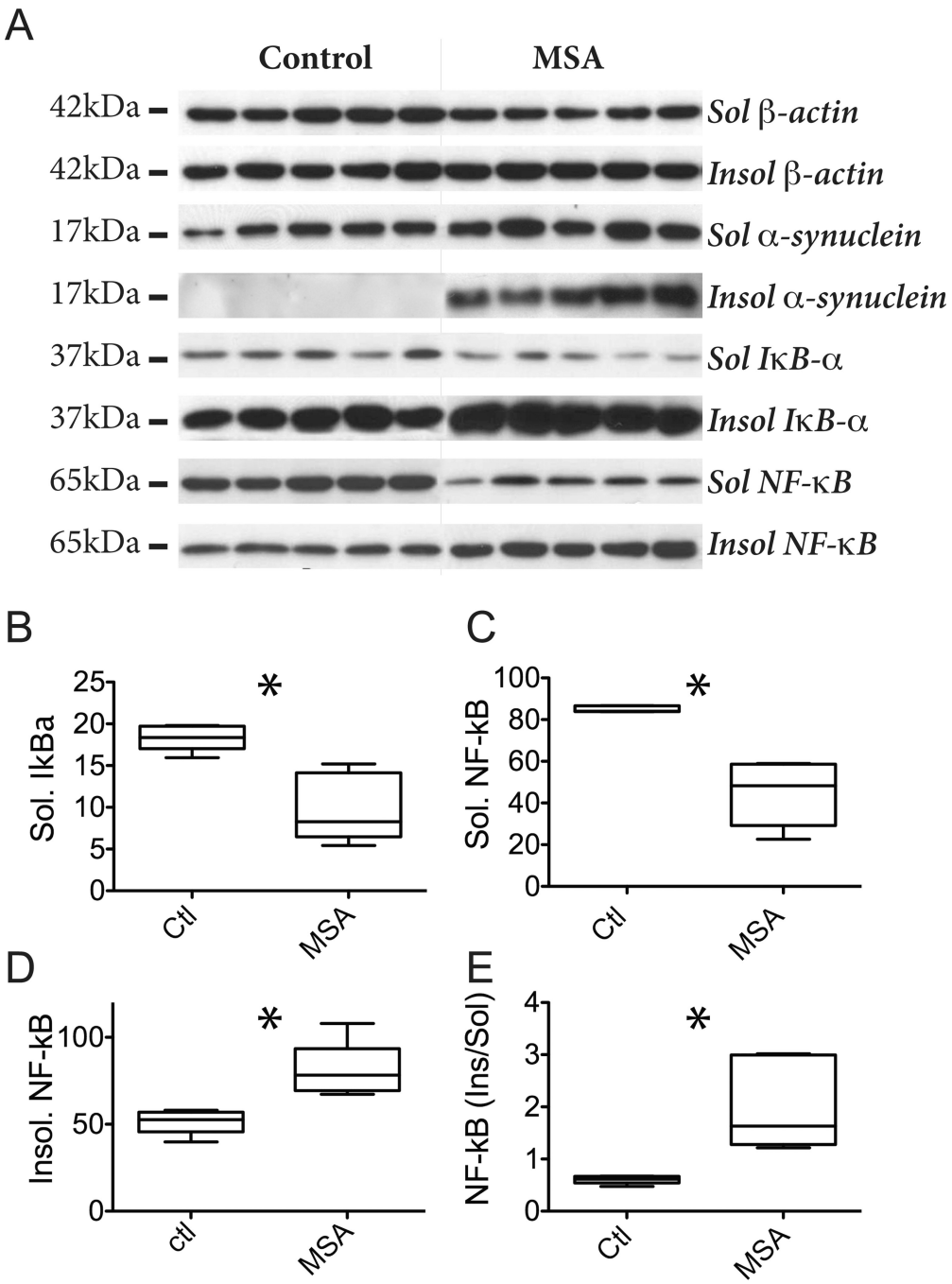

Figure 5. NF-κB and IκBα are increased in MSA white matter

A, Brain tissue (precentral gyrus white matter) from 5 control and 5 MSA patients was fractionated in soluble and insoluble proteins. Insoluble proteins were subsequently solubilized in SDS prior to electrophoretic analysis. Proteins (20 μg) were resolved by SDS-PAGE and analyzed by immunoblotting using antibodies against α-syn, IκBα, and NF-κB p65. β-Actin was included as loading control. The molecular sizes (kDa) of the presented bands are indicated to the left. B–E., The intensities of the individual bands in soluble and insoluble fractions (from A) were quantified and band intensities were normalized to β-actin.

Box plots indicate mean, min, max and S.D. values of the five cases and asterisk indicates significant difference between boxes when analyzed by unpaired t test (two tailed $p < 0.05$). B, Relative amounts of soluble IκBα in control and MSA cases. The 0.54 fold decrease is significant ($p = 0.003$). C, Relative amounts of soluble NF-κB in control and MSA cases. The 0.53 fold decrease is significant ($p = 0.0004$). D, Relative amounts of insoluble NF-κB in control and MSA cases. The 1.55 fold increase is significant ($p = 0.006$)..E, Ratio of insoluble and soluble NF-κB in control and MSA cases. The 3.4 fold increase is significant ($p = 0.007$).

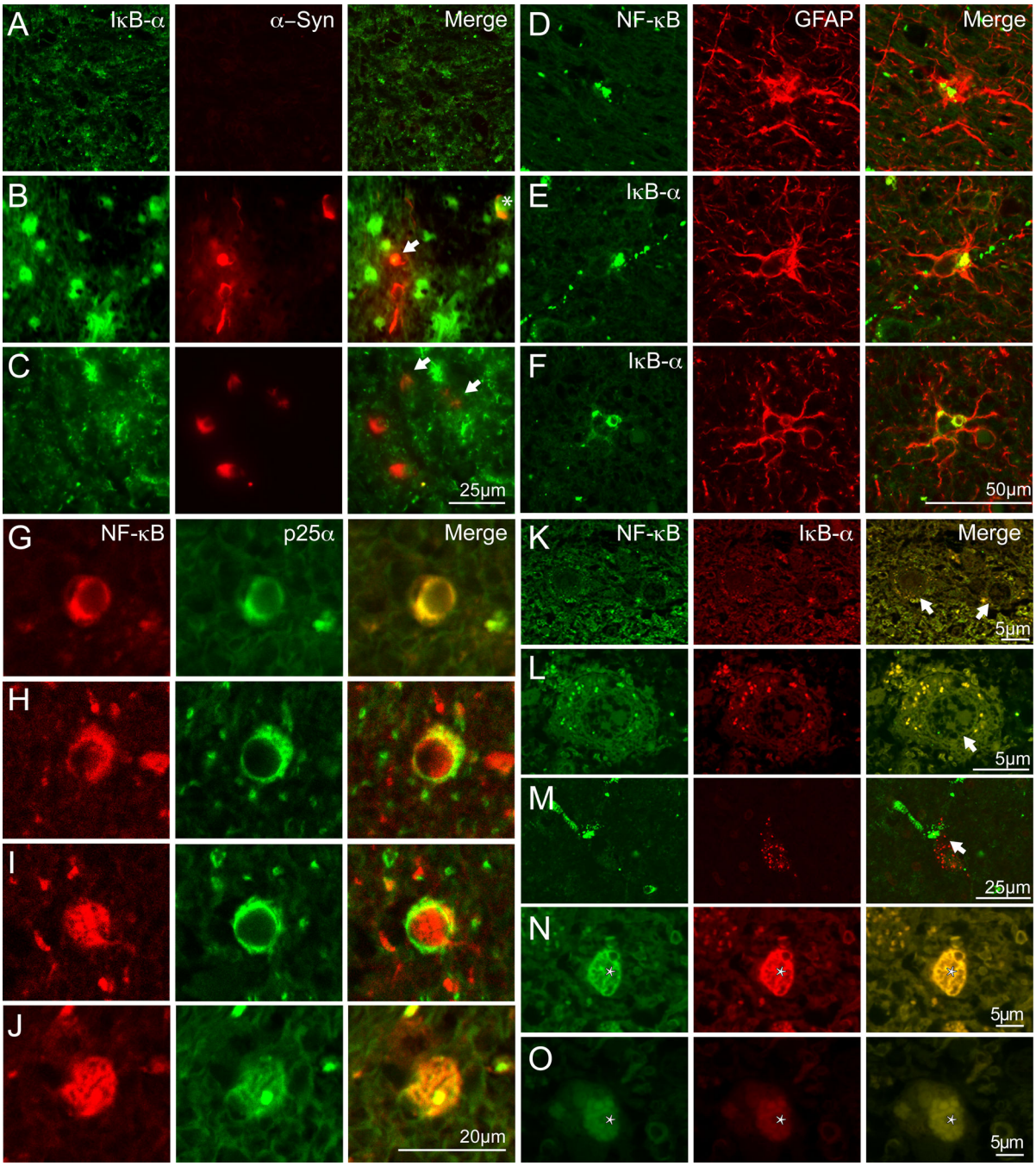

Figure 6. NF-κB and IκBα in brain cells in MSA white matter

A–C, Double labeling immunofluorescence using IκBα (green) and α-syn (red) in pontine white matter of an autopsy confirmed case without neurological or neuropathological abnormalities (A) and an MSA case (B and C). Protein co-localisation is shown in yellow. Limited IκBα and no α-syn immunoreactivity is observed in control pontine white matter whereas high expression of IκBα was observed in reactive astrocytes (bright green cells) in MSA tissue. Low expression of IκBα was observed in a proportion of α-syn immunopositive GCIs (identified by arrow) (B and C). Oligodendroglia with IκBα

immunopositive nuclei had stronger IκBα expression associated with α-syn immunopositive GCIs (GCI colocalising α-syn and IκBα with IκBα immunopositive nucleus is identified by asterisks in panel B) The majority of IκBα was in astrocyte-like cells (B and C). Scale bar, 25 μM.

D–F, Double labeling immunofluorescence using NF-κB (green, D) and IκBα (green, E and F) and GFAP (red) in pontine white matter of an autopsy confirmed MSA case demonstrate the expression of both antigens in astrocytes. Scale bar, 50 μm.

G–J, Double labeling immunofluorescence using NF-κB (red) and p25α (green) in pontine white matter of an autopsy confirmed MSA case demonstrate the expression of both antigens in oligodendrocytes. In the expanded cell bodies of the MSA oligodendrocytes does NF-κB colocalized with the p25a positive GCI of both the early perinuclear type (G–I) and the mature type protruding away from the nucleus. Scale bar, 20 μm.

K–O, Double labeling immunofluorescence using NF-κB (green) and IκBα (red) in pontine white matter of an autopsy confirmed case without neurological or neuropathological abnormalities (K) and a confirmed MSA case (L–O). Granular cytoplasmic colocalization of NF-κB and IκBα in oligodendrocytes that is enhanced in MSA (K vs L) and the colocalization also exists in some nuclei (N–O). NF-κB and IκBα does not colocalize in neurons (M). Scale bar, 5 μm (K and L), 25 μm (M–O).

Table 1

Gene expression changes in response to coexpression of α-synuclein and p25α

Fold changes for selected genes regulated at 8, 12, and 16 h after transfection compared to respective controls (cells transfected with empty vector for 8, 12, and 16 h) along with the reference gene NADH. Fold changes were calculated using MAS 5.0 software (Affymetrix).

Gene symbol	Gene name	Fold Change		
		8 h	12 h	16 h
Iκ Bα (Nfkbia)	Nuclear factor of kappa light chain gene enhancer in B-cells inhibitor, alpha	2.5	3.4	3.5
IL6	Interleukin 6	3.3	6.7	6.7
Bbc3/PUMA	Bcl-2 binding component 3/p53 upregulated modulator of apoptosis	1.6	2.2	2.3
Egr-1	Early growth response 1	3.6	6.5	7.1
NADH	NADH dehydrogenase	1.0	1.1	1.0